JOURNAL OF Materials CHEMISTRY

Dynamic segregation phenomena during oxidation of titanium ferrites

Bruno Domenichini,* Pascal Perriat, Jérôme Merle, Karine Basset, Nadine Guigue-Millot and Sylvie Bourgeois

LRRS, UMR 5613 CNRS-Université de Bourgogne, 9, avenue A. Savary, BP 400, 21011 Dijon cedex, France. E-mail: byhan@satie.u-bourgogne.fr

Received 9th November 1998, Accepted 1st March 1999

The cationic composition of three types of titanium ferrite $Fe_{2.5}Ti_{0.5}O_4$ has been analyzed by XPS during their oxidation in order to reveal dynamic segregation phenomena. These samples included two pulverised materials obtained by high energy ball milling followed by a thermal treatment under a well controlled reducing atmosphere (**I**) and by a ceramic process followed by grinding (**II**), as well as a compact material obtained by a ceramic process (**III**). In each case, under pure oxygen and under a linear increase of the temperature, the material was subject to oxidation in the cation deficient phase *i.e.* without phase transformation below 350 °C. During this reaction, an important modification of the chemical composition of the near surface layers has been revealed: the titanium ferrite surface becomes richer in iron and poorer in titanium. For pulverised compounds, if the heating is extended above 400 °C, the oxidation in a cation deficient phase can proceed and some titanium can move back to the surface. Then, from this temperature, the amount of titanium detected by XPS increases. For samples obtained by high energy ball milling, this phenomenon can lead to a homogeneous compound. This is not so for the samples obtained by the ceramic process. For these, a phase transformation of the compound appears which generates α-Fe_2O_3 at the surface of the material. The segregation phenomenon has been interpreted on the basis of the different mobilities of the species Fe^{2+}, Fe^{3+}, Ti^{4+} and cation vacancies present in the material.

1 Introduction

Mixed solid oxides are materials in which segregation phenomena can be observed. In these compounds, two important types of segregation can be distinguished.[1]

The first type involves chemical segregation of elements because of thermodynamic considerations.[2–4] Such a segregation which occurs at free surfaces, grain boundaries and macrodefects is due to a decrease in free energy: the segregation which occurs at equilibrium depends on the differences in binding energies of crystal atoms at the surface and in the bulk due to the local environment. In this case, the segregation ranges over some atomic layers in depth[5] and the mobility of the elements in the segregation region determines the kinetics of segregation.[6–8]

The second important kind of segregation results from kinetic factors and is denoted 'dynamic segregation'. This kind of phenomenon can be the result of a change in the thermodynamic conditions at the material surface (temperature, gas composition, *etc.*).[9–16] This change induces a new equilibrium state for the material. This new equilibrium state can generate a new composition of the material at the surface first. In this case, a concentration gradient develops between the surface and the bulk and, in order to set up this new equilibrium state (*i.e.* a new composition) in the whole sample, some elements attempt to diffuse. Under these conditions, if, for example, one of the elements which has to migrate from the bulk to the surface cannot diffuse, segregation is observed. This effect can have technological implications.[17]

This study has been carried out in order to clearly reveal this kind of phenomenon. With this aim, a well known compound with a specific crystallographic structure has been chosen: the titanium ferrite $Fe_{2.5}Ti_{0.5}O_4$ which contains different cations (Fe^{2+}, Fe^{3+}, Ti^{4+}) located in two different crystallographic sites: tetrahedral (or A) sites and octahedral (or B) sites. At low temperature (<800 °C) and under oxygen ($P_{O_2}>1$ Pa) this compound, as with most ferrites, is not in thermodynamic equilibrium. Indeed, all the iron cations have to be of valence +3 for this to be so and the structure is metastable. Under these conditions, the material is susceptible to oxidation. Then, two kinds of oxidation can be observed: with or without phase transformation. For small crystal sizes (diameter lower than 1 μm) and at low temperatures (generally lower than 450 °C) the ferrites can oxidize without phase transformation, *i.e.* as a cation deficient phase.[18] The kinetics of such a reaction are governed by the chemical diffusion of the oxidizable cations.[19,20] In this case, because of possible differences in cation mobilities, segregation can be generated.

The aim of this work was to follow the concentration of each element on the surface of three different samples during their oxidation of the cation deficient phase. The evolution of the cation contents during the reactions allowed an investigation of the segregation phenomenon with respect to the different cation mobilities.

2 Experimental

Three types of titanium ferrites, samples **I**–**III**, have been prepared.

The first synthesis route is mechanical activation which consists of milling starting precursors and then annealing ground powders at low temperature to avoid grain growth.[21]

The starting powders are anatase titanium dioxide (Degussa) and iron(III) oxide (TCR). Continuous grinding was performed in a planetary ball mill (Fritsch Pulverisette 7) with a powder to ball weight ratio $R=1/20$. The grinding tools were made of steel (Fe–13%Cr), the volume of the vial was *ca.* 45 cm^3 and seven balls of diameter 13 mm were used. The powders, in stoichiometric proportions, and balls were introduced in the vial under air atmosphere and they were milled for 8 h. The mechanical activation was followed by a reducing treatment at 500 °C for 3 h under an O_2 pressure of 1.4×10^{-24} Pa obtained from suitable N_2–H_2–H_2O gas mixtures and air-cooled.[22] The crystallite size of as-obtained powders was *ca.* 45 ± 5 nm and the samples were well crystallized.

The second type of sample was synthesized by means of a ceramic process. In this method the synthesis consists of a solid–solid reaction between various oxide powders (α-Fe_2O_3,

TiO_2) and metallic iron previously homogenized in appropriate molar ratios according to eqn. (1).

$$Fe_2O_3 + 0.5\ TiO_2 + 0.5\ Fe \rightarrow Fe_{2.5}Ti_{0.5}O_4 \quad (1)$$

The reactant oxide mixture was introduced into a silica ampoule which was degassed and sealed under vacuum (10^{-3} Pa). The sealed ampoule was placed into a programmable furnace at 1170 °C for 4 h then quenched in water to room temperature. The grain sizes were in the range 5–40 μm. In order to enhance the reactivity, the samples were subjected to dry grinding in an agate mortar for 10 min. The grain size decreased to 200 nm, and the size of the particles was homogeneous.

The third type of sample was obtained by a very similar route to the second but the same reactant oxide mixture was first pressed under 15 MPa in order to obtain compact slices of diameter 13 mm. These slices were then introduced in a silica ampoule and subjected to the same treatment. The result was very dense (99%) sintered Ti-ferrite slices.

The different global oxidation ratios were controlled by thermal gravimetry. The samples (20 mg for the powders and *ca.* 100 mg for the slices) were oxidized in a Setaram TGA 24 microbalance under different oxygen pressures with a linear increasing temperature rate (*e.g.* 2 °C min^{-1}) or in isothermal conditions. The reaction was stopped at different temperatures by quenching the samples in order to perform X-ray diffraction or XPS analysis of the compounds at different stages of the oxidation reaction.

The X-ray photoelectron spectroscopy experiments were performed using a Riber MAC2 instrument equipped with an Al anode which was operated at an acceleration voltage of 12 kV with an emission current of 25 mA (300 W). Emerging photoelectrons were analysed with the detector normal to the surface. Spectra were recorded around the 2p peaks for Fe and Ti with a total resolution of *ca.* 1.2 eV. After smoothing, the backgrounds were removed by a Shirley routine[23] as illustrated in Fig. 1. Then, the total area of the $2p_{1/2}$, $2p_{3/2}$ and satellite peaks for both Fe and Ti [A(Fe) and A(Ti)] were measured. This allowed the calculation of the Ti : Fe atomic ratio according to eqn. (2)

$$\frac{Ti}{Fe} = \frac{k_{Ti}}{k_{Fe}} \times \frac{A(Ti)}{A(Fe)} \quad (2)$$

where k_{Ti} and k_{Fe} are Ti and Fe sensitivity factors respectively. Sensitivity factors were obtained from ionization cross sections multiplied by $1/(E_{kin})^{1/2}$ where E_{kin} is the photoelectron kinetic energy.[24] The attenuation of the photoelectron [$\propto (E_{kin})^{1/2}$] and the spectrometer transfer functions ($\propto 1/E_{kin}$) were then taken into account.

X-Ray diffraction analyses were performed with an INEL CPS 120 diffractometer which uses the Kα radiation of a Co anticathode.

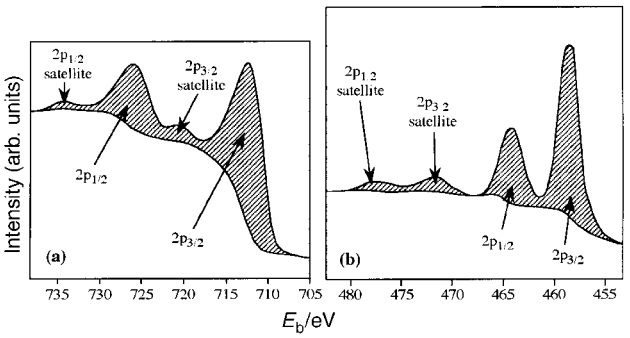

Fig. 1 Principles for XPS quantitative analysis: example of spectra [Fe (a) and Ti (b)] for $Fe_{2.5}Ti_{0.5}O_4$ **I** obtained by high energy ball milling and oxidized under pure oxygen up to 590 °C. The dashed zones correspond to the $2p_{1/2}$ and $2p_{3/2}$ peaks and satellites after background removal using the Shirley procedure and represent the areas used for quantification.

3 Results and discussion

The X-ray data obtained for the three types of ferrite show that for each preparation the compounds were pure and had the spinel structure.

In a first approach, the evolution of the cationic surface composition induced by oxidation was studied for the three $Fe_{2.5}Ti_{0.5}O_4$ samples for a reaction carried out up to 650 °C under pure oxygen ($P_{O_2} = 100$ hPa) with a linear increase of temperature (2 °C min^{-1}). This reaction was followed by thermal gravimetry and X-ray diffraction after different oxidation times (*i.e.* temperature). It has been shown that the sample (**I**) obtained by the high energy ball milling process is oxidized in two steps:[19] the iron(II) ions located in octahedral sites are oxidized between 60 and 220 °C and the iron(II) ions located in tetrahedral sites are oxidized between 200 and 420 °C (Fig. 2). If the oxidation is carried out in a cation deficient phase below 650 °C, no phase transformation is detected. These results are consistent with those established by Gillot *et al.*[25,26] by thermal gravimetry and conductivity analyses on nanometric samples synthesised by soft chemistry.

For the pulverised sample (**II**) obtained by the ceramic process followed by grinding, the iron(II) ions located in octahedral sites oxidize between 100 and 275 °C and the iron(II) ions located in tetrahedral sites between 240 and 600 °C (Fig. 2). The beginning of the reaction is on the cation deficient phase but from 450 °C a phase transformation to α-Fe_2O_3 is detected by X-ray diffraction.[27] In the case of the sintered slices (**III**), the oxidation is detectable only from 400 °C with a phase transformation leading to α-Fe_2O_3. Below this temperature, X-ray data show that the compound conserves its spinel structure, that is to say no structural transformation is observed by X-ray analysis. The oxidation temperatures observed from ground and sintered samples are in accordance with the oxidation temperatures observed by Readman and O'Really[28] from differential thermal gravimetric analyses.

For each type of sample, the Ti/Fe atomic ratio has been determined at different stages of the oxidation reaction with the aid of XPS (Fig. 3). Up to 350 °C the surfaces of all the samples are richer in iron and poorer in titanium. At 350 °C titanium is absent from the surface of material **I** obtained from high energy ball milling. Moreover, if the reaction is

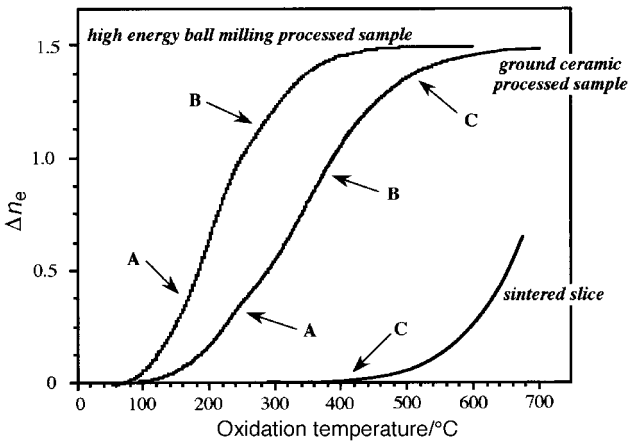

Fig. 2 Quantification of the oxidation of three $Fe_{2.5}Ti_{0.5}O_4$ samples ($P_{O_2} = 100$ hPa; linear temperature increase rate = 2 °C min^{-1}); Δn_e is the amount of electrons exchanged between Fe^{2+} and oxygen for one formula unit; A: oxidation of Fe^{2+} ions located in octahedral sites, B: oxidation of Fe^{2+} ions located in tetrahedral sites, C: phase transformation to α-Fe_2O_3.

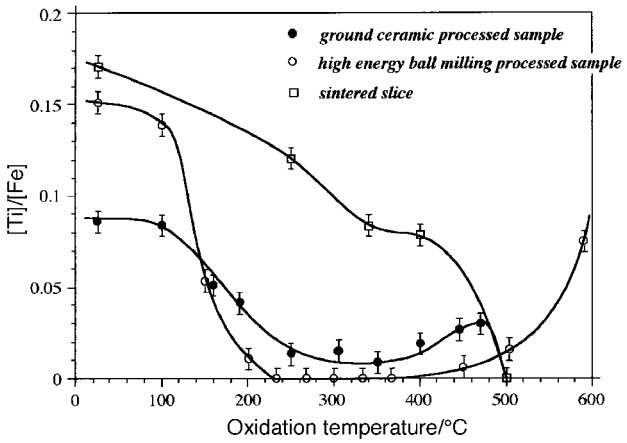

Fig. 3 Evolution of the titanium/iron ratio determined by XPS analysis on the surface of three $Fe_{2.5}Ti_{0.5}O_4$ samples during their oxidation (P_{O_2} = 100 hPa; linear temperature increase rate = 2 °C min^{-1}).

extended above 400 °C, some titanium returns to the surface, in particular for the pulverised samples. However, for the two types of samples **II** and **III** obtained by the ceramic process, the segregation phenomenon leads to a phase transformation: heating at temperatures above 500 °C leads to α-Fe_2O_3 formation as detected by X-ray diffraction, and only iron cations can be detected by XPS (Fig. 3).

These observations can be interpreted from kinetic considerations. Under oxygen pressure the oxidation process begins by dissociative oxygen adsorption on the surface of the particles. This induces an electronic exchange between the surface Fe^{2+} ions and the oxygen atoms [Fig. 4(a)]. These two rapid steps generate Fe^{3+} ions and cation vacancies on the surface of the material and thus composition gradients between the surface and the bulk [Fig. 4(b)]. These gradients do not generate any crystallographic transformation but induce the diffusion of the different cations: Fe^{3+} ions and cation vacancies have to diffuse from the surface to the bulk and Fe^{2+} ions and Ti^{4+} have to diffuse from the bulk to the surface. These diffusion steps govern the oxidation process. Nevertheless,

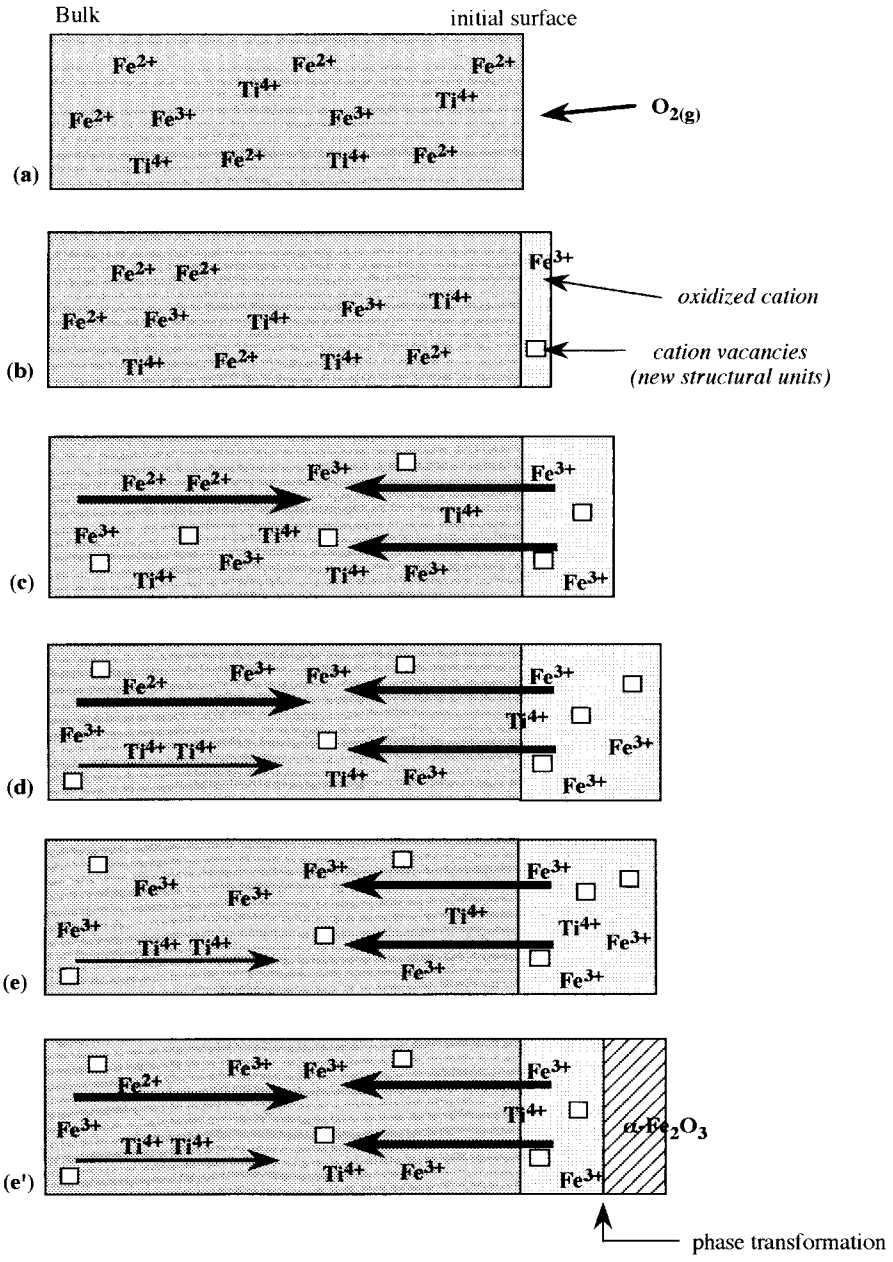

Fig. 4 Scheme of the pulverised $Fe_{2.5}Ti_{0.5}O_4$ oxidation mechanism during a linear temperature increase: (a) the initial non-oxidized metastable ferrite, (b) the oxidized compound at room temperature, (c) below 350 °C, (d) at *ca.* 400 °C, (e) at *ca.* 450 °C and (e′) above 500 °C for the ground ceramic processed sample **II**.

because Ti^{4+} is a high valence ion, it is strongly bound to the oxygen anions and consequently its mobility is lower than that of iron ions. Under these conditions, at the begining of the reaction, Ti^{4+} cations cannot diffuse to the surface.

The segregation phenomenon is a function of the degree of the oxidation reaction. Since the reaction already occurs at room temperature, even at 25 °C no sample has a titanium/iron ratio on the surface equal to 0.2, the theoretical value for a homogeneous material (Fig. 3). Moreover, the low 'initial' titanium/iron ratio recorded for the pulverised sample **II** synthesized by the ceramic process can be explained by the effect of the grinding which induces a significant preoxidation of the material.[29]

The three different samples have different macroscopic oxidation reaction rates (Fig. 2). Nevertheless, the amount of adsorbed oxygen atoms on the material surface per unit area is the same for each material. Indeed, the reaction rate differences result principally from differences in specific surface and particle sizes. Under these conditions, if the number of new structural units generated per unit area is the same for all samples, the segregation phenomenon has to be the same for all three ferrites. However, the segregation rates are very different (Fig. 3): the phenomenon is fastest for the smallest sized particles. This can be explained by the strong stresses which are present in small sized ferrite grains.[20] Such stresses speed up the beginning of oxidation in a cation deficient phase while for large particles, the stresses are lower, the oxidation reaction is slower and consequently the segregation phenomenon is slowed down.

In order to further the understanding of the segregation phenomenon other experiments have been performed: a sample pre-oxidized at 350 °C was submitted to long annealing under nitrogen pressure (in order not to change the global oxidation state) either at 350 °C or at 400 °C. The results are presented in Fig. 5 for the ground ceramic processed sample **II**. For the 350 °C annealing no change of the XPS Ti/Fe ratio could be observed: below 350 °C Ti^{4+} cations cannot diffuse [Fig. 4(c)] and thus no titanium ions can migrate to the surface. However, upon annealing at 400 °C, an increase of the XPS Ti/Fe ratio is observed: above 400 °C, the titanium mobility is now significant and Ti can migrate to the surface [Fig. 4(d) and (e)]. It should be noted that this appearance of titanium ions at the surface is observed for the ground ceramic and soft chemistry processed samples as evidenced in Fig. 6. In the particular case of the sample **I** obtained by high energy ball milling, 10 h annealing at 600 °C of a totally oxidized compound leads to a homogeneous material. However for the sintered slices **III**, the return of the titanium to the surface cannot be observed because of the transformation of the compound below 400 °C.

The above results can allow an estimate of a rough value for the iron–titanium interdiffusion coefficient. From such an estimate, we can conclude that titanium cannot diffuse below 400 °C. Then, in the case of the samples obtained by high energy ball milling, below 400 °C we can anticipate the formation of a hypothetical pure iron oxide layer on the sample surface. The depth of this layer can be easily estimated with the help of the formalism of oxidation reactions in a cation deficient spinel as previously suggested.[30] Oxidation of $Fe_{2.5}Ti_{0.5}O_4$ can be written in terms of eqn. (3)

$$(Fe_{1.5}{}^{2+}Fe_{0.5}{}^{3+}Ti_{0.5}{}^{4+})O_4{}^{2-} + 0.375\ O_{2(g)} \rightarrow 1.19\ (Fe_{2.11}{}^{3+}Ti_{0.42}{}^{4+}\square_{0.47})O_4{}^{2-} \quad (3)$$

where □ represents a cation vacancy.

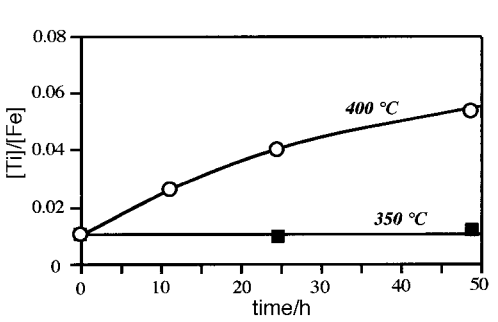

Fig. 5 Evolution of the titanium/iron ratio on the surface of the material during isothermal treatment at two temperatures under N_2 for pulverised $Fe_{2.5}Ti_{0.5}O_4$ sample **II** obtained by the ceramic process (oxidation at 350 °C under O_2) followed by grinding.

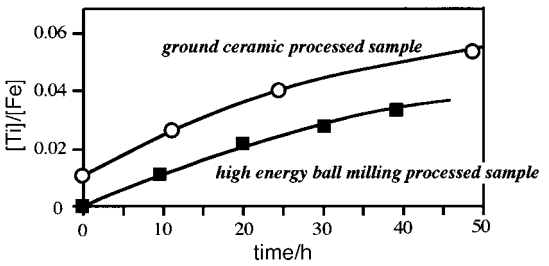

Fig. 6 Evolution of the titanium/iron ratio on the surface of the material during an isothermal treatment at 400 °C under N_2 for two pulverised $Fe_{2.5}Ti_{0.5}O_4$ samples **I** and **II** which have been previously oxidized at 350 °C under O_2.

This depiction of the reaction is not realistic since the oxidation does not lead to a homogeneous compound. However, it allows an estimate of 19% for the increase in the crystal volume. This volume increase corresponds to a radius increase of *ca.* 6%, *i.e.* for the high energy ball milling sample, about 3 nm. As 10 h annealing at 600 °C of a totally oxidized and inhomogeneous compound leads to a homogeneous material, we can estimate that the time for 3 nm interdiffusion is *ca.* 10 h. This result can be compared with those obtained by Freer and Hauptman[31] at high temperatures and low titanium content: *viz.* 216 days for 2 μm interdiffusion, *i.e.* 7.8 h for 3 nm interdiffusion!

For samples **I** and **II** obtained by the ceramic process, a phase transformation reaction is detected after the total oxidation of the material: above 500 °C the α-Fe_2O_3 phase is evidenced by X-ray diffraction. Moreover, in this case, only iron cations can be detected by XPS (Fig. 3) and the α-Fe_2O_3 phase screens the ferrite surface [Fig. 4(e′)]. This is a consequence of the segregation phenomenon. Indeed, the transformation temperature of a metastable ferrite to a stable α phase is a function of the cations which are present in the spinel structure.[19] For example, Ti^{4+} ions stabilize the spinel structure[32] and the transformation temperature of an oxidized Ti-ferrite is higher than the transformation temperature of the maghemite γ-Fe_2O_3 (*i.e.* oxidized Fe_3O_4). Now, because of segregation during the oxidation, the composition of the external part of the ferrite is close to γ-Fe_2O_3. Under these conditions, the γ→α reaction begins on the surface where there is a low amount of Ti^{4+}. As Ti^{4+} cannot be incorporated in α-Fe_2O_3, the transformation reaction generates pure α-Fe_2O_3 on the surface of the material which screens the ferrite. Thus, titanium ions cannot be detected by XPS.

The γ→α reaction is a function of the ferrite particle size.[33] This could explain why the small grain samples obtained by high energy ball milling undergo transformation. The compounds synthesized by the ceramic process contain defects resulting from the quenching and the grinding. Under such conditions the metastability of the spinel structure is lower and a transformation is observed prior to total oxidation of the material.

5 Conclusion

This study has revealed important dynamic segregation phenomena during the oxidation of titanium ferrites. This

segregation results from the oxidation mechanism and is a consequence of the differences in mobilities between the cations. Taking into account these phenomena is very important in understanding the whole process which occurs during an oxidation reaction in cation deficient phases.

It should be noted that the dynamic segregation processes lead to a material with composition gradients which can have a high thermal metastability. This gradient can induce high stresses in the bulk[20] and then can induce particular properties in the material. For example, in the case of cobalt ferrites, high stresses induce a high coercivity.[34] Correct understanding of the phenomenon allows selection of appropriate treatments (oxidation and annealings at selected temperatures, substitution of elements by more or less mobile ones, *etc.*) leading to a material having a specific composition gradient inducing the desired properties.

References

1 J. Nowotny, I. Sikora and J. B. Wagner, Jr, *J. Am. Ceram. Soc*., 1982, **65**, 192.
2 J. Nowotny, *Mater. Sci. Forum,* 1988, **29**, 99.
3 J. Nowotny, *Surfaces and Interfaces of Ceramic Materials*, ed. L. C. Dufour, C. Monty and G. Petot-Ervas, Kluwer Academic Publishers, Dordrecht, 1989, p. 205.
4 W. D. Kingery, *J. Am. Ceram. Soc*., 1974, **57**, 1.
5 H. Matzke, *Surfaces and Interfaces of Ceramic Materials*, ed. L. C. Dufour, C. Monty and G. Petot-Ervas, Kluwer Academic Publishers, Dordrecht, 1989, p. 241.
6 J. Crank, *The Mathematics of Diffusion*, Clarendon Press, Oxford, 1975.
7 C. Lea and M. P. Seah, *Philos. Mag*., 1977, **35**, 213.
8 J. Du Plessis and E. Taglauer, *Surf. Sci*., 1992, **260**, 355.
9 H. Schmalzried, W. Laqua and P. L. Lin, *Z. Naturforsch.*, *Teil A*, 1978, **34**, 192.
10 M. Martin and H. Schmalzried, *Ber. Bunsen-Ges. Phys. Chem*., 1985, **89**, 89.
11 D. Dimos, J. Wolfenstine and D. L. Kohlstedt, *J. Am. Ceram. Soc*., 1987, **70**, 531.
12 T. Ishikawa, S. A. Akbar, W. Zhu and H. Sato, *J. Am. Ceram. Soc*., 1988, **71**, 513.
13 G. Petot-Ervas and C. Petot, *J. Eur. Ceram. Soc*., 1988, **71**, 513.
14 J. Wolfenstine, D. Dimos and D. L. Kohlstedt, *J. Am. Ceram. Soc*., 1985, **68**, 117.
15 H. Schmalzried, *React. Solids*, 1986, **1**, 117.
16 B. Domenichini, C. Vautrein, S. Petigny, K. Basset, S. Bourgeois and A. Steinbrunn, *Mater. Chem. Phys.*, 1998, **55**, 209.
17 F. Armanet, H. Klimczyk, D. Monceau, C. Petot and G. Petot-Ervas, *High Temp. Sci*., 1991, **31**, 147.
18 B. Gillot, F. Jemmali, C. Clerc and A. Rousset, *React. Solids*, 1986, **2**, 95.
19 B. Gillot and A. Rousset, *Heterog. Chem. Rev*., 1994, **1**, 69.
20 P. Perriat, B. Domenichini and B. Gillot, *J. Phys. Chem. Solids*, 1996, **57**, 1641.
21 N. Millot, S. Beguin-Colin, P. Perriat and B. Le Caer, *J. Solid State Chem*., 1998, **139**, 66.
22 D. Aymes, N. Millot, V. Nivoix, P. Perriat and B. Gillot, *Solid State Ionics*, 1997, **101–103**, 261.
23 D. A. Shirley, *Phys. Rev. B*, 1972, **5**, 4709.
24 J. H. Scofield, *J. Electron Spectrosc. Relat. Phenom*., 1976, **8**, 129.
25 B. Gillot, F. Jemmali, L. Clerc and A. Rousset, *C. R. Acad. Sci. Paris*, 1986, **302**, 211.
26 B. Gillot, F. Jemmali and A. Rousset, *J. Solid State Chem.*, 1988, **72**, 209.
27 K. Basset, B. Domenichini, J. Merle, P. Perriat and S. Bourgeois, *Eur. Phys. J. AP*, 1998, **4**, 157.
28 P. W . Readman and W. O'Really, *Phys. Earth Planet. Inter.*, 1970, **4**, 121.
29 B. Gillot, B. Domenichini and P. Perriat, *Solid State Ionics*, 1996, **84**, 303.
30 B. Gillot, B. Domenichini and A. Rousset, *Ann. Chim. Fr.*, 1993, **18**, 175.
31 R. Freer and Z. Hauptman, *Phys. Earth Planet. Inter.*, 1978, **16**, 223.
32 B. Gillot, F. Jemmali, C. Clerc and A. Rousset, *React. Solids*, 1986, **2**, 95.
33 F. Mathieu, P. Roux, G. Bonel and A. Rousset, *C. R. Acad. Sci. Paris*, 1987, **299**, 781.
34 E. Kester, B. Gillot and P. Tailhades, *Mater. Chem. Phys*., 1997, **51**, 258.

Paper 8/08732F